

Polymer Communication

Probing the urea hard domain connectivity in segmented, non-chain extended polyureas using hydrogen-bond screening agents

Sudipto Das^a, Iskender Yilgor^b, Emel Yilgor^b, Garth L. Wilkes^{a,*}

^a Department of Chemical Engineering, Macromolecules and Interfaces Institute, Virginia Tech, Blacksburg, VA 24061, United States

^b Department of Chemistry, Koc University, Istanbul, Turkey

Received 15 August 2007; accepted 17 October 2007

Available online 4 November 2007

Abstract

The effects of long-range connectivity between urea hard domains on the microphase morphology and mechanical properties of novel, segmented, non-chain extended polyureas based on single isocyanate molecules were analyzed. This was achieved by systematic disruption of the intermolecular bidentate hydrogen bonding between the urea hard segments by the incorporation of a hydrogen bond screener, LiCl. A systematic decrease in the breadth of the service temperature window and mechanical properties of the polyureas were observed in the presence of LiCl, due to the disruption of the long range connectivity between the hard segments. The above mentioned effects were also found to be dependent on the symmetry of the diisocyanate hard segments.

© 2007 Published by Elsevier Ltd.

Keywords: Hydrogen-bonding; Polyurea; Microphase

1. Introduction

Thermoplastic polyurethanes (TPUs) are segmented copolymers containing alternate hard and soft segments (SSs). While the SSs provides flexibility, the hard segments (HSs) act as physical crosslinks, thereby enabling melt processibility of these materials, unlike conventional crosslinked elastomers. The SSs of most commercially available TPUs are based on aliphatic polyester, polyether or polycarbonate oligomers. HSs are produced through the reactions of diisocyanates and chain extenders (such as low molecular weight diols). For the last few years, we have been working on novel segmented, *non-chain extended* polyurethanes and polyureas, which are synthesized by a one-step synthesis of either dihydroxy- or diamine-terminated poly(tetramethylene oxide) (PTMO) oligomers with stoichiometric amounts of various symmetric and asymmetric diisocyanates [1–6]. While the SSs of these segmented copolymers are based

on PTMO, the HSs are only based on *a single molecule of the diisocyanate* used. Results indicated that even with very low HS contents (*ca.* 6 wt% for copolymers based on 2000 g/mol PTMO), most of the segmented copolyureas showed the presence of a distinctly microphase-separated morphology, where the hard domains formed thin thread-like structures that were dispersed throughout the soft PTMO matrix.

The properties of both of these segmented thermoplastic polyurethanes and polyureas (TPUs) were found to be significantly affected by the symmetry of the HS. Copolymers with symmetric HSs were found to possess a significantly broader thermal service window (often referred to as the service temperature window, STW) and higher modulus and tensile strength than the corresponding asymmetric counterparts. The hydrogen-bonding capabilities of the HSs also influenced the properties of these segmented copolymers, such as the polyureas with bidentate hydrogen-bonding showed a significantly broader STW, better microphase separation and mechanical properties than the corresponding polyurethanes with monodentate hydrogen-bonding [1,3,5]. The properties of these segmented polyureas were also found to be affected by the

* Corresponding author. Tel.: +1 540 231 7867; fax: +1 540 231 5044.

E-mail address: gwilkes@vt.edu (G.L. Wilkes).

PTMO molecular weight. The polyureas with higher PTMO molecular weights (2000 g/mol) were found to show greater SS crystallinity at sub-ambient temperatures, narrower STW but surprisingly similar tensile properties, i.e. similar stress and strain at break values [2] relative to the corresponding lower PTMO molecular weight (1000 g/mol) polyureas. While both the high and low PTMO molecular weight polyureas showed the presence of a microphase-separated morphology (from AFM analysis), long-range connectivity between the hard domains was only strongly observed for the lower PTMO molecular weight polyurea (from uniaxial deformation experiments). The time-dependent morphological development (after heat treatment above the respective HS melting temperature) of selected polyurethanes was also studied with transmission FTIR spectroscopy which showed that the structure of the HS had dramatic effects on the kinetics and amount of microphase separation [6]. Meijer et al. [7] and Gaymans et al. [8,9] have also reported on segmented, non-chain extended copolymers with uniform HSS', which show similar phase-separated morphology like our systems.

As indicated earlier, the properties of segmented thermoplastic copolymers, such as TPUs and TPUrs are known to originate from the presence of a microphase-separated morphology which in turn is driven by the presence of hydrogen-bonding between the hard segments [10–12]. The role played by hydrogen-bonding in mediating the long-range connectivity of the hard domains in segmented, non-chain extended polyureas and how it affects their morphology and mechanical properties may be probed by the systematic incorporation of an “additive” that can preferentially disrupt the bidentate hydrogen-bonding between the urea HSs and alter the microphase separation and/or connectivity between the HS domains in these materials. For example, lithium salts are known to disrupt hydrogen-bonding in polymers and have been used in the past to form “softer” polyurethane-urea (PUUr) foams with high HS contents [13] and to modify the performance of polyamide polymers [14]. Several studies have been undertaken in our laboratory in the past to understand the role of urea phase connectivity in addition to the microphase separation on the mechanical properties of flexible PUUr foams, molded flexible foams and model trisegmented oligomeric PUUr, by using various lithium halides (LiCl and LiBr) as molecular probes [13,15–19]. As just stated, the materials in these earlier investigations were novel model trisegmented PUUr copolymers, which were chain extended with water. Results showed that incorporation of lithium halides (up to 1.5 pph based on polyol) led to a reduction of the physical association of the urea aggregates (macro connectivity) and disruption of the regularity of segmental packing of urea HS (micro connectivity) [15]. This in turn affected the morphology, as noted from the systematic breakdown of hard domains observed by AFM [17,19] and mechanical properties such as the systematic softening of model polyurethanes [19] and higher rates of stress relaxation in flexible slabstock PUUr foams [15].

The present study involves analysis of the hard-segment connectivity in two different segmented, *non-chain extended*

polyureas, whose HS are based on a single molecule of either 1,4-phenylene diisocyanate (*p*-PDI, symmetric HS) or a 80/20 mixture of 2,4- and 2,6-toluene diisocyanate (TDI, asymmetric HS), by systematic incorporation of LiCl and characterization of the resultant morphology and mechanical properties of the polyureas. It was anticipated that this study would allow us to obtain further information and understanding of the contribution of hydrogen-bonding in mediating the long-range connectivity of monodisperse urea-based HS in our polyureas, but without the presence of any chain extenders.

2. Experimental

2.1. Materials

1,4-Phenylene diisocyanate (*p*-PDI), α,ω -aminopropyl terminated poly(tetramethylene oxide) ($M_n = 1100$ g/mol) and LiCl were purchased from Aldrich. A 80/20 mixture of 2,4- and 2,6-toluene diisocyanate (TDI) was kindly provided by Bayer, Germany. Reagent grade dimethylformamide (DMF) was purchased from Aldrich and used as received.

2.2. Copolymer synthesis

All copolymers were prepared by reacting equimolar amounts of a selected diisocyanate and amino-terminated PTMO oligomer in DMF at room temperature. Detailed discussion of the full synthesis of these segmented copolymers is provided in previous reports [1,3].

2.3. Fabrication of LiCl-doped polyurea films

Anhydrous LiCl (2 wt% based on solution) was dissolved in DMF. Measured amounts of various polyurea samples were dissolved in DMF (15 wt% based on solution). Then various levels of LiCl–DMF solutions were added to the polyurea solution, which was then stirred in a stoppered flask at 60 °C overnight. The amounts of LiCl added to the various polyurea samples are shown in Table 1. After complete dissolution of the polyurea, the solutions were poured into a Teflon mold and the solvent was evaporated at 60 °C for 24 h, followed by 24 h under vacuum (30 mm Hg) at room temperature. Sample films were stored under dry conditions until tested.

2.4. Characterization methods

Dynamic mechanical analysis was performed on a Seiko DMS 210 tensile module with an auto-cooler for precise

Table 1
LiCl content in various segmented, non-chain extended polyureas films

LiCl added		Number of LiCl molecules per urea linkage	
wt% based on solution	wt% based on polyurea	TDI	<i>p</i> -PDI
0.1	0.7	0.012	0.010
0.2	1.4	0.022	0.020
0.3	2.0	0.032	0.030

temperature control. Samples were cut (12 mm in length and 4–6 mm in width) from cast film and deformed (1 Hz frequency, 10 μm amplitude) under a dry nitrogen atmosphere. The temperature was increased from $-150\text{ }^{\circ}\text{C}$ to $300\text{ }^{\circ}\text{C}$, at a heating rate of $2\text{ }^{\circ}\text{C}/\text{min}$.

The phase images of the samples were obtained by performing AFM analysis on the free air side of the solvent-cast films. The analysis was conducted at ambient conditions and within 30 min to minimize the moisture absorption. AFM images were obtained using a VEECO Dimension 3000 atomic force microscope with Nanoscope IIIA controller. Images were obtained under ambient conditions using Nanodevices TAP150 silicon cantilever probe tips (5 N/m spring constant, $\sim 100\text{ kHz}$ resonant frequency). The free air amplitude was normally set at 2.8 V and the set point ratio was varied between 0.4 and 0.7, which constituted hard to medium tapping, respectively.

The stress–strain behavior of the samples was measured on a Instron Model 4400 Universal Testing System controlled by Series IX software. Dog-bone shaped samples (with 10 mm gauge length and 2.91 mm width) were cut from solvent-cast films using a standard bench-top die. Samples were deformed under ambient conditions at a cross-head speed of 25 mm/min until failure occurred.

The hysteresis behavior of the samples (dog-bone shaped with the above mentioned dimensions) was also recorded. Samples were deformed to 300% strain (25 mm/min cross-head speed) and then brought back to its initial conditions (0% strain), at the same cross-head speed. Each sample was subjected to four loading–unloading cycles.

FTIR analysis was performed on a MIDAC M2004-ATR system, under ambient conditions. Spectra of solvent-cast polyurea films were collected at a resolution of 4 cm^{-1} and 64 scans were co-added to each file. Background scan of similar nature was performed before each sample scan.

3. Results and discussion

The polyurea samples were doped with three different levels of LiCl to systematically disrupt the bidentate hydrogen-bonding between the urea HS of two different polyurea samples (based on symmetric *p*-PDI and asymmetric TDI HSs). The asymmetry of TDI HSs originated due to the presence of two different (2,4- and 2,6-) isomers. The number of LiCl species per urea linkage in the two polyureas studied is shown in Table 1. Previous studies [1,3] have shown that even with only 13 wt% HS content, both *p*-PDI and TDI polyureas possessed microphase-separated morphology where the HSs formed thread-like domains that were dispersed throughout the soft PTMO matrix. While the HS threads were found to be crystalline in nature (from WAXS analysis), with long-range connectivity between the hard domains in the *p*-PDI polyurea, the hard domains in the TDI polyurea sample were found to be amorphous in nature and devoid of any long-range connectivity [1,3]. Detailed description of the morphology and mechanical properties of these two polyureas are presented in past reports [1,3].

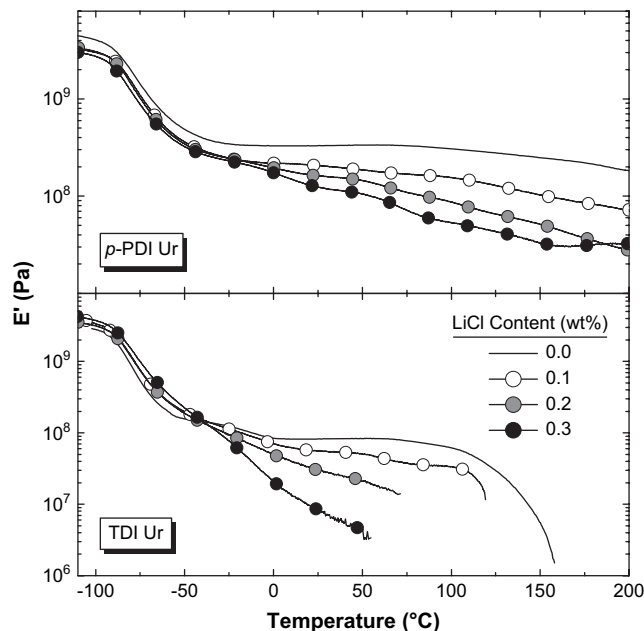


Fig. 1. Effect of LiCl incorporation on the DMA spectra of two different segmented, non-chain extended polyureas.

The effect of LiCl incorporation on the temperature-dependent modulus of the polyurea samples was initially analyzed by DMA (Fig. 1). Both the asymmetric (TDI) and symmetric (*p*-PDI) polyurea control samples (i.e. without LiCl) showed a relatively flat temperature-independent STW with a relatively high modulus (*ca.* 10^8 Pa) at $25\text{ }^{\circ}\text{C}$. The rubbery plateau modulus of *p*-PDI ($3.3 \times 10^8\text{ Pa}$) was slightly higher than the corresponding asymmetric polyurea based on TDI ($8.2 \times 10^7\text{ Pa}$). The high rubbery plateau modulus observed for segmented copolymers with such low HS content (*ca.* 13 wt%) is due to the presence of a microphase-separated morphology where the HSs formed thin thread-like structures that percolated throughout the soft PTMO matrix with long-range connectivity between the hard domains [1,3]. Incorporation of LiCl was shown to result in a systematic decrease in the ambient rubbery plateau modulus of the polyureas, which is attributed to the loss of long-range connectivity between the urea hard domains (also confirmed by performing ambient AFM analysis, which is presented later in this report) as observed in previous studies [15,18,19]. Addition of LiCl, not surprisingly, also led to a systematic decrease in the breadth of the STW, which was most distinctly observed for the asymmetric TDI polyurea system. The latter observation may be ascribed to the increased disruption of the interchain hydrogen-bonding between the segmented polyureas with LiCl addition, which in turn increases the ease of HS–HS chain slippage at higher temperatures. The overall effect of LiCl was also found to be more pronounced in the asymmetric TDI polyurea relative to its symmetric counterpart. For example with incorporation of 0.3 wt% LiCl, while the rubbery modulus of the TDI dropped to $8.7 \times 10^6\text{ Pa}$ (90% decrease), the *p*-PDI polyurea had a modulus of $1.2 \times 10^8\text{ Pa}$ (60% decrease). Readers might be tempted to ascribe this effect to the slightly greater LiCl content in TDI polyurea compared to the corresponding *p*-PDI polyurea

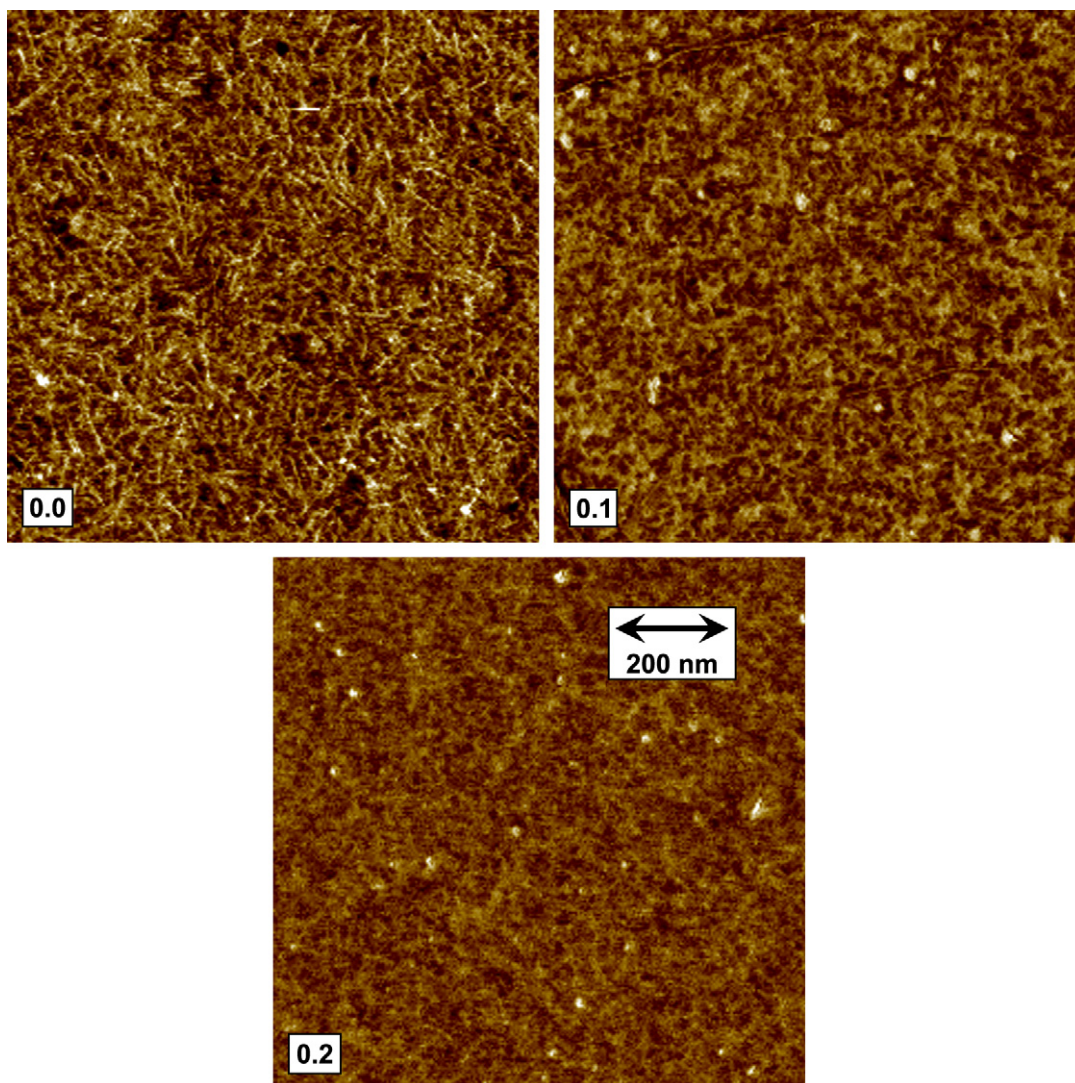


Fig. 2. Tapping mode AFM phase images of TDI Ur containing various levels of LiCl (scale bar applies for all micrographs).

(Table 1), but we postulate it to be due to symmetry effects as will be shown later in this paper.

As mentioned previously, the effect of LiCl addition on the surface morphology of the polyureas was analyzed by tapping mode AFM and shown in Fig. 2 for TDI polyurea. As the LiCl content was increased, a systematic breakdown of the urea hard domain connectivity was observed in the form of a decrease in the length of the thread-like HSs. A similar effect, i.e. loss in contrast between hard domains and soft PTMO matrix and decrease in the density of the even more distinct thread-like hard domains, was also observed in the *p*-PDI polyureas samples, but is not shown in this report. This also led to softening of the polyurea samples under ambient conditions, as exemplified by reduced ambient modulus of the polyurea samples in their DMA traces (Fig. 1). The TDI polyurea sample with 0.3 wt% LiCl was also found to be quite soft and tacky and as a result of which it could not be analyzed by tapping mode AFM (it contaminated the AFM tips during analysis). The changes in the morphology of the polyureas as analyzed by AFM were again found to be more pronounced in TDI relative to *p*-PDI polyurea.

The effect of LiCl incorporation on the hydrogen-bonding capabilities was analyzed by ATR-FTIR spectroscopy by observing the changes in the absorption spectra specifically in the C=O ($1600\text{--}1750\text{ cm}^{-1}$) stretching bands (Fig. 3).

Previous studies [20] have shown that this region has contributions from “free” ($1710\text{--}1715\text{ cm}^{-1}$), monodentate hydrogen-bonded ($1700\text{--}1650\text{ cm}^{-1}$) and bidentate hydrogen-bonded ($1640\text{--}1650\text{ cm}^{-1}$) C=O stretching vibrations. Both the undoped polyurea samples showed a single sharp absorption peak at *ca.* 1635 cm^{-1} due to the bidentate hydrogen-bonded C=O stretching vibration. Incorporation of LiCl led to a systematic decrease in the intensity of the bidentate C=O stretching vibration along with the increase in the intensity of monodentate hydrogen-bonded C=O stretching vibration (1670 cm^{-1}). Similar trends were also observed in the *p*-PDI polyurea samples but the effects were found to be less disruptive relative to the corresponding TDI polyurea samples. This showed that under similar conditions, it was easier for LiCl to disrupt the domain structure of the polyureas based on asymmetric hard segments.

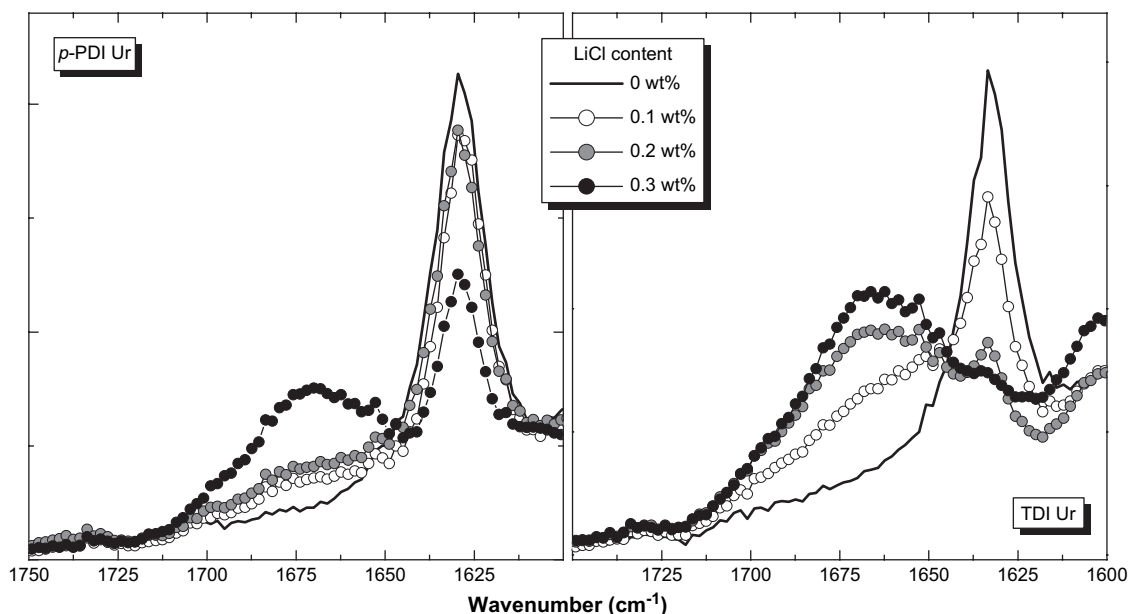


Fig. 3. Effect of LiCl on the FTIR spectra of the segmented, non-chain extended polyureas (each spectrum was normalized with respect to the PTMO C–O–C stretching at 1105 cm^{-1}).

The effect of LiCl incorporation on the mechanical properties of the segmented, non-chain extended polyureas was also analyzed at ambient conditions by performing mechanical hysteresis measurements (Fig. 4). Results showed that with addition of LiCl, there was a systematic drop in modulus and tensile strength along with a systematic decrease in the mechanical hysteresis and instantaneous set (Table 2). The undoped segmented *p*-PDI polyurea sample showed the presence of a small, but distinct yield point in their stress–strain curves suggesting long-range connectivity between the hard domains. However, the yield point was absent in all the LiCl-doped *p*-PDI polyurea samples which indicated that though all the samples possessed a microphase-separated morphology, the

Table 2

Ambient mechanical hysteresis results for segmented, non-chain extended polyureas

Urea	LiCl added (wt% solution)	Mechanical hysteresis (%)		Instantaneous set (%)
		1st cycle	2nd cycle	
<i>p</i> -PDI	0	87	56	150
	0.1	84	58	134
	0.2	79	49	115
	0.3	76	51	90
TDI	0	83	60	138
	0.1	81	43	132
	0.2	71	47	85
	0.3	70	55	—

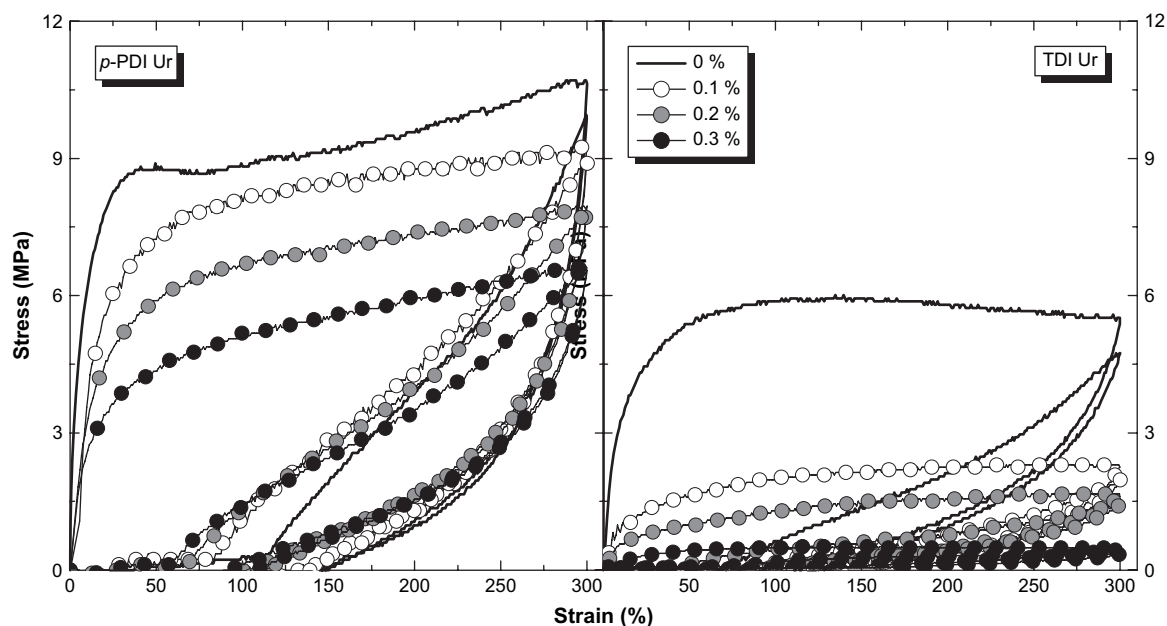


Fig. 4. Effect of LiCl on the ambient, mechanical hysteresis of the segmented, non-chain extended polyureas.

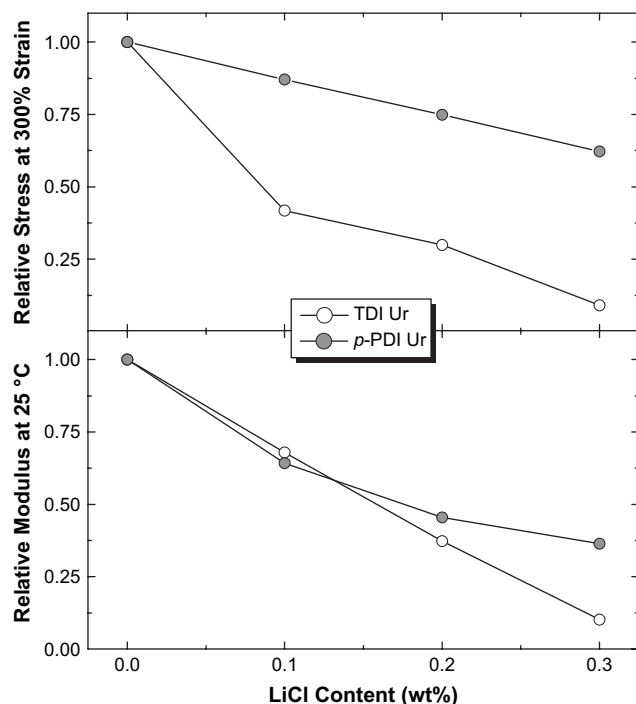


Fig. 5. The relative changes in the ambient modulus obtained from DMA and ambient stress at 300% strain obtained from uniaxial tensile testing of the *p*-PDI and TDI polyurea samples due to incorporation of hydrogen-bond screening agent, LiCl.

long-range connectivity between the hard segments was reduced and disappeared in the more highly doped samples. This loss in long-range connectivity also led to decrease in the instantaneous set observed in both these samples.

The effect of incorporation of LiCl on the morphology and mechanical properties of the two segmented, non-chain extended polyureas was found to depend on the symmetry of the HS. Results presented above showed that the changes in the polyurea morphology and decrease in the intermolecular hydrogen-bonding between the urea HSs with the incorporation of similar amounts of LiCl were greater in the asymmetric polyurea relative to the symmetric polyurea. Fig. 5 also shows that while both the symmetric *p*-PDI and asymmetric TDI (due to the presence of different isomers) showed a decrease in the ambient modulus and stress at 300% strain, the effect was significantly more in the polyurea consisting of the asymmetric HS. All these observations pointed to the fact that it was relatively easier for the LiCl to disrupt the intermolecular hydrogen-bonding between the asymmetric HSs relative to their symmetric counterparts as exemplified by the larger decrease in the hydrogen-bonded C=O intensity in the asymmetric polyureas (Fig. 3).

4. Conclusions

The role played by hydrogen-bonding in mediating the long-range connectivity of the hard domains in segmented, non-chain

extended polyureas was probed by the systematic incorporation of a hydrogen-bond screening agent, LiCl. Results showed that in the range of LiCl content investigated, the intermolecular hydrogen-bonding between the urea HSs decreased systematically, which in turn led to a systematic decrease in the mechanical properties of these segmented polyureas. Even in the presence of LiCl, all the polyureas showed evidence of a microphase-separated morphology but the long-range connectivity between the urea HSs was found to be distinctly absent, based on the disappearance of yield point in uniaxial deformation experiments. The effect of LiCl incorporation on the morphology and mechanical properties of the polyureas were also found to be dependent of the symmetry of the urea HSs, with asymmetric polyureas being affected relatively more than the corresponding symmetric polyurea.

Acknowledgements

This project was supported by the U.S. Army Research Laboratory and the U.S. Army Research Office under grant number (DAAD19-02-1-0275) Macromolecular Architecture for Performance (MAP) MURI.

References

- [1] Das S, Klinedinst DB, Yilgor I, Yilgor E, Beyer FL, Wilkes GL. *Journal of Macromolecular Science: Physics* 2007;46:853–75.
- [2] Das S, Yilgor I, Yilgor E, Inci B, Tezgel O, Wilkes GL. *Polymer* 2007; 48,(1):290–301.
- [3] Klinedinst DB, Yilgor E, Yilgor I, Beyer FL, Sheth JP, Wilkes GL. *Rubber Chemistry and Technology* 2005;78:737–53.
- [4] Sheth JP, Klinedinst DB, Pechar TW, Wilkes GL, Yilgor E, Yilgor I. *Macromolecules* 2005;38:10074–9.
- [5] Sheth JP, Klinedinst DB, Wilkes GL, Yilgor I, Yilgor E. *Polymer* 2005; 46:7317–22.
- [6] Yilgor I, Yilgor E, Guclu Guler I, Ward TC, Wilkes GL. *Polymer* 2006; 47(11):4105–14.
- [7] Versteegen RM, Kleppinger R, Sijbesma RP, Meijer EW. *Macromolecules* 2006;39:772–83.
- [8] Krijgsman J, Feijen J, Gaymans RJ. *Polymer* 2004;45:4677–84.
- [9] Krijgsman J, Feijen J, Gaymans RJ. *Polymer* 2004;45:4685–91.
- [10] Cooper S, Tobolsky AV. *Textile Research Journal* 1966;36(9):800.
- [11] Schollenberger CS. *Handbook of elastomers*. New York: Marcel Dekker Inc.; 2001. p. 387.
- [12] Schollenberger CS, Scott H, Moore GR. *Rubber Chemistry and Technology* 1962;35:742.
- [13] Moreland JC, Wilkes GL, Turner RB, Rightor EG. *Journal of Applied Polymer Science* 1994;52:1459–76.
- [14] Wu Y, Xu Y, Wang D, Zhao Y, Weng S, Xu D, et al. *Journal of Applied Polymer Science* 2004;91:2869–75.
- [15] Aneja A, Wilkes GL. *Polymer* 2002;43:5551–61.
- [16] Aneja A, Wilkes GL. *Polymer* 2004;45:927–35.
- [17] Aneja A, Wilkes GL, Yilgor E, Yilgor I, Yurtsever E. *Journal of Macromolecular Science: Physics* 2003;B42(6):1125–39.
- [18] Aneja A, Wilkes GL, Yurtsever E, Yilgor I. *Polymer* 2003;44:757–68.
- [19] Sheth JP, Wilkes GL, Fornof A, Long TE, Yilgor I. *Macromolecules* 2005;38:5681–5.
- [20] Kaushiva BD, McCartney SR, Rossmly GR, Wilkes GL. *Polymer* 2000;41:285–310.